A Review paper of 3D Surface Reconstruction of Coronary Arteries From Cardiovascular Angiography

Hasan H. Khaleel[1,*], Rahmita O. K. Rahmat[1], DM. Zamrin[2], Ramlan Mahmod[1], Norwati Mustapha[1]
[1]Department of Computer Science and Information Technology, Universiti Putra Malaysia, 43400, Serdang, Selangor, Malaysia
[2]Heart and Lung Centre, National University of Malaysia Medical Centre, PPUKM, 56000, Cheras, Kuala Lumpur, Malaysia
[*]hassan.upm@gmail.com; rahmita@fsktm.upm.edu.my; drzamrin@gmail.com; ramlan@fsktm.upm.edu.my; norwati@fsktm.upm.edu.my

***Abstract*—This paper begins with a review of the coronary artery trees extraction techniques within different eras. Next, a review of 3D reconstruction of coronary artery trees approaches is presented in details. A well presentation of the center of gravity approaches is included within the 3D reconstruction review techniques. Finally, the paper discusses the surface reconstruction techniques throughout their development stages. Each stage of the review paper is concluded by a summary. This paper is concluded by a comprehensive summary which discussed the lack of a robust approach in each stage of it. The improvement of a new approach in each stage depends on the lack in that stage and the results which are expected from the work.**

Keywords- angiography; coronary artery trees extraction; 3D reconstruction; center of gravity; surface reconstruction.

I. INTRODUCTION

This paper is aimed at presenting the previous technical elements and algorithms in a literature review of the a PhD thesis entitled "3D Surface Reconstruction of Coronary Arteries From Cardiovascular Angiography to Detect Location of Heart Vessels". The paper starts with a block diagram to show the sequence of approaching the literature review. The block diagram is shown in Fig. 1 below. Next, the review focuses on the four technical approaches that have been used in this paper which are coronary artery tree extraction, 3D reconstruction, centre of gravity in 3D data, and surface reconstruction. Finally, the paper is concluded in a summary.

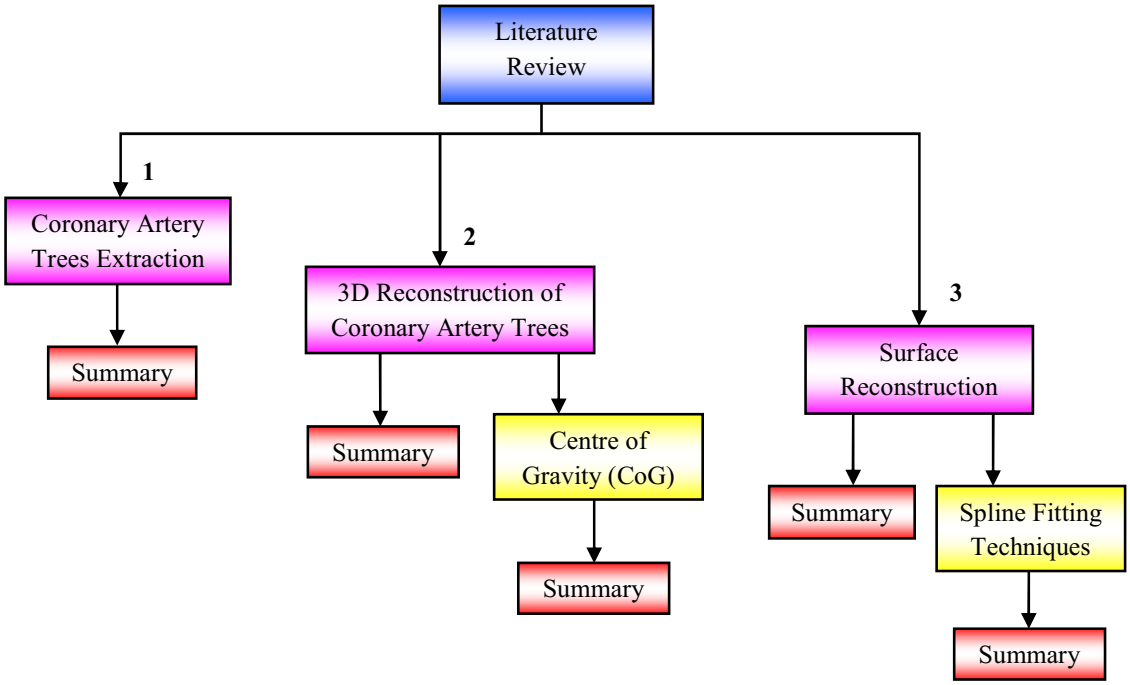

Figure 1. Block diagram showing the sequence of approaching the literature review of this paper.

978-0-7695-4959-0/13 $25.00 © 2013 IEEE
DOI 10.1109/ACSAT.2012.13

II. CORONARY ARTERY TREES EXTRACTION

Coronary artery tree extraction is the process of extracting vascular artery networks from 2D angiocardiography (angiogram) images. The output for the extraction process is a binary tree of vessels with main arteries as well as bifurcations. This process is a vital step in the work of this paper since it is the first step of pre-processing of our dataset angiogram images to highlight the objects required from them and remove the background. A tremendous amount of work has been done in the field of vessel extraction and the procedures have taken different ways. Some of the previous work focused on tracking the centreline of the vessels and other algorithms were interested in extracting the contours of the blood vessels. In addition, the previous methods and approaches worked with different types of medical images such as ultrasound, MRI or MRA, CT scans, and a few others as well as angiograms.

The reason behind the small amount of work handling angiograms as a dataset is the functionality of angiograms, i.e., the drift in image intensity and the poor signal-to-noise ratio. Despite the big challenge, angiograms are still much preferred by modern physicians because they can do the diagnosis procedure online and check the diseases of arteries in real-time. In addition, there has been very little previous work that focused on extracting the vessels of coronary artery trees as a full package of centreline, contours, and items in between such as the work proposed in [1, 2]. The previous algorithms addressed the problem of vessel extraction in three categories. The first category used the geometrical topology information of images to extract the blood vessels. Meanwhile, the second category utilized the intensity value of pixels to handle the extraction. The last category combined the geometry and intensity information. Blood vessel extraction techniques and algorithms have been divided into six main categories since the beginning of interest in research in this field as reported in the survey paper of [3]. Some of the categories are further divided into sub-categories as well. The categories and sub-categories are shown in Table I below. The same main categories were reported also in [4] with implemented examples. The previous work reported here was applied to different types of medical images. A thorough search among those approaches and methods helped us to produce the algorithm used to extract coronary artery trees in this paper. In general, a visual inspection of coronary angiograms suffers from inherent imprecision that has led to the development of the semi - and fully - automatic tools that apply computerized techniques for image analysis to the assessment of coronary artery disease.

TABLE I. CATEGORIES OF BLOOD VESSEL EXTRACTION TECHNIQUES AND ALGORITHMS

Category	**Pattern recognition**	**Model-based**	**Tracking-based**	**Artificial Intelligence-based**	**Neural Network-based**	**Tube-like object detection**
Sub-category	Multi-scale	Deformable models	/	/	/	/
	Skeleton-based	Parametric models	/	/	/	/
	Region growing	Generalized cylinders	/	/	/	/
	Ridge-based	/	/	/	/	/
	Geometry-based	/	/	/	/	/
	Matching filter	/	/	/	/	/
	Mathematical morphology	/	/	/	/	/

All the previous work included under algorithms and approaches are listed in Table I and the following were evaluated for some suitable approaches previously undertaken in this field. One of the earliest theses reporting edge detection in images in [5]. This work covered the problem of changing intensity in images and it has become canonical in the study of vision. The papers in [6, 7] reported the use of kernels of matched filters to segment an image according to the pattern recognition category. This work used a technique called sequential edge linking which could search for any possible artery boundaries within a range. The algorithm reported good results of accurately extracting coronary artery dimensions. Chaudhuri et al. in [8] addressed the problem of extracting blood vessels from retina images. Retina images, similar to angiograms, have a poor signal-to-noise ratio and conventional edge detection methods do not always produce acceptable results to extract the features from this type of image. This work introduced an operator for feature extraction and the gray level is enhanced by a Gaussian filter. The results were good for detecting vessels in retina images but the method consumes time on ordinary computers, therefore, it needs a special computer with special specifications.

One of the best methods in the field of tracking the centreline of a vessel was advocated in [9]. The dedicated algorithm tracked the centreline and extracted the contours by exploiting the diameter and intensity of a vessel. The algorithm was automatic and used the geometric parameters of the vessels and was guided by a matched filter but it needed a start-to-search point to start the tracking process. Computer simulation was also used to explain the overall arterial tree structure. A model was built on the computer to present a vascular tree grown by adding several segments. This type of work could be a helpful tool to compare the presented computerized model with the real arterial trees in terms of appearance. One of the main goals of vessel extraction in the previous algorithms was the local features. Vessels can be precisely characterized by their curvilinearity (shape) and gradient which represent the strength of the boundary, and the level of contrast with their background. The features and image manifestations, including optic nerves and boundaries, could possibly show similar features as vessels such as reported in [10]. The classification of vessels depends on window-based techniques to track such vessels. The drawback of this kind of technique is that vessels usually have large-scale features, and therefore this approach cannot be applied until the preliminary segmentation of vessels has been undertaken. This problem makes it impossible to distinguish the features to derive the segmentations or even to perform an evaluation.

Meanwhile, intensity methods involve pixel labeling such as in [11] which has been adopted by some researchers who focused on tubular object segmentation and registration depending on the intensity ridge and widths as in [12]. The work explained how to handle noise using optimal and multi-scale measurements on CT scan, MRA, and ultrasound 3D images. The work was fast and accurate but needed more refinement in terms of boundaries estimated by ridges and widths. Matched filter approaches have taken up much space in the field of vessel extraction because of the high response that could be obtained from different types of medical images. The algorithms were distinguished by fast response and accurate output. Therefore, a large number of researchers still have interest to enhance the previous algorithms and to develop new algorithms to improve the vessel extraction field and enrich it with new ideas. One such researcher who developed an algorithm which used a matched filter response to locate blood vessels in retina images was [7]. The functionality and features of retina images tend to be different from other types of images and a matched filter was a necessary technique to determine the local and global features of blood vessels in the eye. The method yielded good results by reducing the false positive detection rate by 15 times over the basic thresholding technique. This algorithm inspired us to research further into this area as it indicated good possibilities for improvement.

The tremendous amount of work in vessel extraction research suffers from a lack of evaluation tools that can show and prove the correctness of the algorithms. Therefore, creating tools to evaluate and simulate the real-world was considered highly necessary in this field. Few researchers have tried to accomplish this mission of creating a simulation tool to generate angiography images to imitate the real world. One of the notable algorithms in this area was in [13] and has been used to evaluate centreline extraction accuracy in Quantitative Coronary Angiography (QCA) images. This algorithm presented an understanding of the relationship between the performance and limitations of centreline algorithms and the geometrical parameters of vessels. The algorithm was used to evaluate the work of [9] as one of its applications and gave good results. Another centreline extraction method was defined in [14] which was based on a previous report from 1996. The Monte Carlo method was used with a clinical dataset to evaluate the speed, accuracy, and automation of the algorithm with the challenge of dealing with a high level of noise.

Vessel extraction is a required technique in different fields, including 3D visualization. The algorithm presented in [15] explained an efficient method for skeleton extraction from angiography images by analyzing the quantitative features of the vessels. The method reported good results and less sensitivity to noise. It is worth mentioning that medical images link classical diagnostic procedures with modern treatment. This current study requires the use of image segmentation to detect objects to be segmented. In this area, the work in [16] presented a semi-automatic skeleton-based approach for vessel segmentation in CT scans of 3D datasets of images. The algorithm was reliable for extracting coronary arteries but the searching needed to be supplied with start and end points to track the centreline path. The same year witnessed another work to extract blood vessels in noisy retina video images in [17]. Three mathematical modelling methods were used to solve this problem relying on intensity, width, orientation, scale, and noise of images. The method was robust in terms of vessel detection and the performance depended on the level of false positives that could be tolerated.

The work in [3] presented a signal-based algorithm for coronary artery identification in X-ray angiography. The algorithm was described as robust and used different techniques and filters to extract arteries in poor signal-to-noise images. The techniques of 3D Fourier and 3D wavelet transform were employed to reduce noise and background, after which a matched filter was used to enhance the output. Wang et al. presented in [18] a method to extract centrelines and the contours of coronary arteries in Digital Subtracting Angiography (DSA) images. The method demonstrated efficient extraction in a short time period but only on DSA images. Another algorithm presented coronary artery tree extraction from poor quality angiogram images as put forward in [2]. Their idea was to use a circular sampling method to extract vessels where the segmentation process gave each pixel a different depth on a varying background from 2D slice images. The results showed good performance as an automatic method of extraction of vascular arteries. The drawback of this method was the long processing time it took to extract vessels but the authors suggested using pattern methods or the Monte Carlo method to reduce the processing time.

It was mentioned earlier in this chapter that vessel extraction techniques use different ways to approach the extraction process. Xu et al. presented in [19] an approach which was applied to centreline tracking of vessels using the combined approaches of geometrical and intensity parameters. This method could efficiently handle the difficult situation of vessel complications. A region-based active contour model algorithm was proposed in [20] to overcome the intensity inhomogenities problem that may occur in images. The algorithm can draw an active contour model in local regions upon intensity information and at a controllable scale. The algorithm works in a similar way to region growing approaches whereby an initial contour is given to start the searching process and intensity information is used to grow the contour until object(s) are covered and their contours extracted. The level set function should be preserved to avoid expensive computations and reinitialization protocols.

A few researchers have become involved in 3D angiography segmentation, for example [21], as this is an essential process for diagnosing blood vessel diseases and image analysis. The method in [21] was reported to have a high robustness to noise but it needed starting and ending points to extract the centrelines of vessels. The work in [22] presented an automatic method to detect tubular objects, provide centreline extraction, and perform tree structure building from grouping the single centrelines in CTA images. In their paper, they claimed that their work performed well on vessel detection with centrelines and it was a good start for further research of diameter measurements for stenoses assessment. Finally, [23] proposed an algorithm using line-like features where the extracting procedure was accomplished by a directional filter bank, which they claimed acted better on noisy images to disclose the vessel networks. Unfortunately, although the algorithm in [23] worked better in noisy environments than conventional methods, it was restricted to 2D images and needed further work to extend to 3D images.

A. Summary of the Coronary Artery Trees Extraction

From the previous literature concerning the vessel extraction problem, we have noticed that this issue has been investigated widely and in different ways. However, tremendous amount of researchers have sought to work on specific types of images, such as CTA and MRA, rather than angiography images because of the poor signal-to-noise ratio associated with the latter images. On the other hand, many physicians are seeking angiocardiography images nowadays since such images can offer diagnostic procedures on the spot (online). We feel that further investigation and improvement can be undertaken for angiograms by exploring some of the approaches in the literature, especially that of [7]. Their approach was a robust work on processing retina images and further improvement can be made to derive a new algorithm which can be applied to coronary artery tree extraction taking into consideration that retina images and angiograms share the same characteristic of a poor signal-to-noise ratio.

III. THREE-DIMENSIONAL (3D) RECONSTRUCTION OF CORONARY ARTERY TREES

The 3D reconstruction function is a process of transferring 2D images into 3D objects in the $\boldsymbol{R^3}$ domain. Coronary angiography is used to project the coronary arteries into the 3D space as illustrated in Fig. 2 below. The 3D reconstruction of coronary arteries has proven to have great benefit in the medical field such as studying the diseases that may occur in the arteries. Use of 3D is also important in the regression and progression of diseases that may be seen by the motion of the myocardium, ease the study of overlapping vessels, allow the examination of the wall stresses of the heart, perform catheter-based procedures, and others. Computer assistance has been used to perform 3D imaging of the structure of the coronary arteries in some of the earlier approaches. The 3D reconstruction was performed from the data of 2D projections which means that the difficulties of 3D extraction should be the same. There is a long history of research in this field but it is obvious that most of the investigations solved the problem depending on multi-view projections (biplane and above) such as [24, 25] respectively. The following presents some of the 3D reconstruction algorithms and approaches, after which a summary is given of those 3D approaches.

The research in this field started in the 1970s and has continued until today. A work in 1990, [26], investigated a few of the papers from the 1970s and 1980s and came up with a method of 3D coronary artery structure reconstruction using 2D biplane angiography images. The algorithm depended on the geometrical mathematics of the arterial images and the contrast dye inside the vessels to identify the vessels. The drawback of this algorithm is that an error may occur in the 3D analyses. Sometime later, [24]

presented another algorithm to reconstruct 3D coronary arteries from multiple 2D MRA images (four noisy images). The method was robust for the reconstruction of 3D objects but unfortunately it was time consuming.

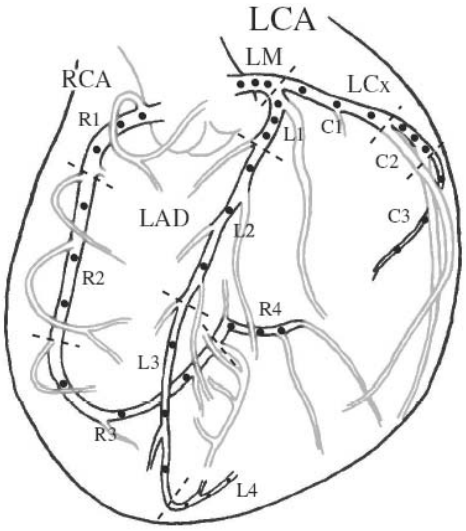

Figure 2. An illustration of a 3D model of the coronary arteries, presented in [37].

Approaches in [27, 28] presented two methods of 3D reconstruction of coronary arteries using biplane angiograms. The first method was generalized by estimating the vessel parameters to compute the elliptic parameters from a nonlinear model in both biplane images. The results of this method showed a good performance for nonlinear modelling over other modalities (derivative-based models). The second method used morphologic analyses of the 3D model as a basis. Morphological analyses produce information such as the shape of a vessel, diameters, lengths, volumes of segments, and branching. The model was helpful in both clinical and research uses. Similarly, a 3D reconstruction of the media axes of coronary arteries using a single-view cineangiogram was presented in [29]. Their proposed method determined the correspondences of artery segments in sequential frames; where the local features have been used. Their results showed a large 3D reconstruction model in about 30 pixels but with an error of 2 pixels which was considered acceptable.

In 1996, [25] presented another algorithm for the 3D reconstruction of heart arteries from biplane angiograms. They proposed a semi-automatic morphology technique to extract vessels in both 2D projections. Some of the researchers moved to another level of the 3D problem investigation in [30]. They presented a method for the curvilinearity structure enhancement of vessels in 3D medical images. Their proposed method focused more on using 3D line filtering and the enhancement of the line characteristics; however, further research was needed as this method was time consuming. Chen and Carroll proposed in [31] a 3D reconstruction method of angiograms from two views. However, most of the traditional approaches require selected views for which overlap and foreshortening is minimized based on 2D projections. This method was adopted to work with an arbitrary two views from any orientation using a single-plane imaging system. The drawback of the algorithm was the issue of the amount of time consumed which could possibly be solved by further research. Another work in [32] proposed a 3D tracking of coronary arterial vessels using sequences of biplane angiographies. The algorithm achieved its goal by depending on the generalizations of deformable models and Fourier descriptors were used for shape representation and were obtained from the 2D descriptors of the projections.

In the same year of 2001, [33] introduced a new algorithm for 3D reconstruction from biplane DSA. The algorithm included three main steps which were multi-resolution segmentation for the coronary vessels, medial axes for the whole artery tree in both views, and the projection of the enhanced reconstruction onto higher multi-resolution medial axes with updating at the higher resolution. They claimed that their algorithm worked better than the available computer simulation models and manual reconstruction but unfortunately, it took a longer time to reconstruct the 3D models. To minimize the foreshortening and overlap of vessels, a quantitative algorithm of 3D reconstruction of a coronary artery tree from more than two 2D views was presented in [34]. The 2D projections were chosen by the angiographer to be at one end - diastole and at the other end - systole; however, there was no way to know the error that may occur in the Quantitative Coronary Angiography (QCA) process.

Meanwhile, [35] presented a method for quantitative measurements of vessel diameters, volumes, and lengths in 3D reconstructed coronary arteries. The method was applied to examine the narrowing that might occur in patients with a clinical exhibition of progressive stenoses. The results were good but further investigation into MRA or ultrasound images would be required. Meanwhile, [36] investigated an algorithm for the 3D reconstruction of a coordinated body surface because of the high increase in the irregular beat (arrhythmia) of the heart using two CT fluoroscopic projections. Their results showed that the reconstructed heart surface was insensitive to the biplane images which were chosen but one of the limitations of the algorithm was the error that may occur at a distance of 10 mm from coronary bypass grafts. In 2004, [37] introduced a model-based approach to recover a scaling index from single plane cineangiograms. Their approach depended on the minimization of Root Mean Square (RMS) distances between a reference point and a projected point from the model. However, they faced some problems in implementation and they suggested that deformable models might not be suitable for this approach.

Most of the previous algorithms focused on reconstructing the coronary trees in 3D except a few which investigated the reconstruction part of the arterial tree. Hoffman et al. presented in [38] a method to reconstruct the carotid arteries in 3D using only a single vessel from two projections. They claimed that their 3D output could be

viewed in less than 1 minute and it was reliable with just the two projections. The method could be a robust way of qualitative and quantitative analyses of the vessels. A study based on Intravascular Ultrasound Images (IVUS) for 3D reconstruction of coronary arteries from biplane images was described in [39]. They claimed that their algorithm gave robust results that could be used in clinical practices on vessel morphology and diffuse arterial diseases. A study of the 3D reconstruction of coronary arteries from a single rotation of X-ray sequence projections was presented in [40]. Their study also presented a 4D coronary artery motion estimation and they claimed that their algorithm gave robust results for reconstructing the coronary arteries in 3D and could be used in clinical practice but the algorithm could be applied for different types of data acquisition especially for holding the breath.

In 2007, an automatic method was introduced in [41] for segmenting micro-CT 3D images. Their method presented a full vascular network that was able to serve as the basis for the artery perfusion. The method was verified using real and synthetic data of a rat and the results were satisfactory. In 2007, [42] described a novel algorithm for 3D visualization of the heart and its coronary arteries. The algorithm included two steps of processing; offline segmentation of the coronary artery images and online application of the transfer function on the gradient value to enhance the tags. The presented algorithm was helpful in diagnosing ischemic heart diseases.

Another algorithm for 3D reconstruction of coronary artery centrelines from two projections of a single rotation of an imaging system was proposed in [43]. The techniques used in [43] are mentioned here briefly. Curve evolution was used to enhance the images, a multi-scale method was used to enhance the arterial structures, the thresholds of the arteries were determined using different quantiles, a thinning procedure was followed to extract the centrelines, pattern recognition techniques were used to remove non-vessels, edge detection was applied, and finally the 2D centrelines compared with a disparity map to extract the 3D model of the centrelines. The intermediate results could be interpreted by a physician yet the processing time was 25.8 seconds for a 512×512 angiogram image which was quite a long processing time.

The 3D reconstruction technique has been used in different fields of life and the medical field is one of the main users. Therefore, different algorithms and approaches have been presented to perform 3D modelling for different objects, i.e., not just coronary arteries. One of the algorithms that were presented in this field was proposed in [44] for 3D reconstruction of the cerebral dilation of vessels from micro-CT scans. The algorithm could reconstruct the dilated vessel with a stent of STL (Steel) format from rotational angiography. The model was useful in 3D reconstruction and computational simulation. The 3D reconstruction algorithms played a vital role in recent tracking of blood flow procedures. The blood flow could be estimated from tracking the contrast dye in the coronary arteries in the image sequences. The behaviour of the coronary arteries could be estimated by using the contrast agent velocity compared to what is called the TIMI frame count (TFC).

A 3D reconstruction algorithm for the TFC was presented in [45] and the reconstruction process was achieved from biplane images. The results of the algorithm and how good or bad the reconstructed segments were depended on the error that was measured. An open platform called *CAVAREV* was presented in [46] to evaluate the 3D and 4D reconstructions of coronary arteries. This algorithm helped in comparing 3D and 4D reconstructions of arterial vessels like the ones obtained from CT scans. Two projection sets can be provided and the intrinsic motion of the two sets can be distinguished from the cardiac motion in both cases, i.e., periodic and non-periodic. The quality of the reconstruction results has been evaluated based on two segmentation quality measures.

A. Summary of the 3D Reconstruction of Coronary Artery Trees

The literature has been investigated for the 3D reconstruction of coronary arteries in different approaches and images. Most of the previous proposed algorithms have investigated the 3D reconstruction from biplane projections and some of them from more than two views. It is worth mentioning that the more views that are obtained, the more exposure to X-ray radiation a patient will get and the more contrast dye that has to be injected. Since, the exposure to X-ray radiation for a long time and the greater the amount of dye injected can cause cancer in patients; therefore, a 3D reconstruction approach using less views would be highly desirable to meet this requirement.

B. Centre of Gravity (CoG)

The centre of gravity or centre of mass is a well-known technique to calculate the centroid or geometric property of any object. It was invented and used for the first time by the United States military with the purpose of finding the centre of gravity of tanks, airplanes, and other military objects. The calculation of CoG was done by averaging the weight of an object as per the procedure given in the website *http://www.grc.nasa.gov*. The motion of any object can be described by translating its CoG to another position and rotating it about its CoG for free rotating objects. The conventional ways of calculating CoG was by calculus and later by a geometrical approach. Geometrical methods proved to have robustness in many cases to calculate the CoG of objects. The determination of the CoG of flying objects is important because of the freedom airplanes and rockets have in rotating around their CoG. If the weight and mass were not uniformly distributed in each part of the object, the calculation of CoG would become more difficult and complicated. Therefore, if the mass is uniformly distributed, the CoG lies on the symmetry line of the object and can be calculated as the average of its physical dimensions. Fig. 3 below illustrates the calculation of CoG for different objects.

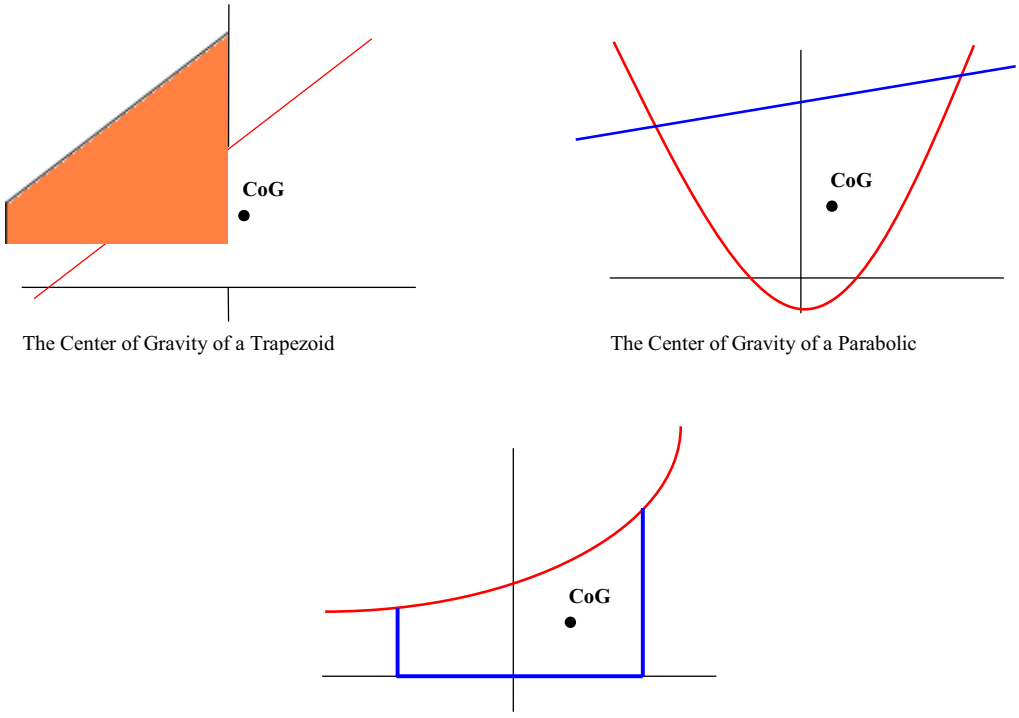

Figure 3. CoG calculation for different regions from [52].

Much research on how to calculate the CoG has been conducted over many years and has been widely used to find the centroid of different objects. Arlot, in [47], explained the technique of measuring the CoG of planets using photographic plates. A few problems were encountered when measuring the CoG of planets on photographic plates due to the asymmetrically and irregularity of such images.

The proposed algorithm in [47] aimed to improve the translation of a planet image to a photographic plate of its CoG. The advantage of such an algorithm was to improve the determination of the coordinates of some planets in order to be more accurate. The algorithm gave good results but with the drawback of being time consuming. Then, [48] presented another algorithm to calculate the CoG for seat wheelchairs with a patient. Using some information like the patient's weight, wheelchair tire coefficients, and some other various assumptions plus the CoG, a method for calculating the rolling resistance of a wheelchair was outlined. This method was helpful to increase the consistency of setting up of wheelchairs and to be more efficient. The centroid of an object as used to assess the accuracy of the measurement of its position to determine the ideal symmetry of an object was investigated in [49]. The position of an object can be estimated by measuring the centroid in a single-dimension (1D), in 2D, and in 3D. By comparison of the results of the 1D, 2D and 3D centroid properties, complete differences could be noticed in the properties. It has been proven in [49] that the accuracy of 3D is higher than the accuracy of 2D and the last one is higher than 1D. The results have shown the advantage of measuring the centroid of objects to increase the accuracy of position determination.

Using the CoG for the determination of geometrical features has been investigated in [50]. The algorithm presented in that research was used to determine the geometrical features of some human face features such as the nose, eyes, and mouth. Some information of those features was used to determine the CoG template which was used to determine the face location. The algorithm was considered fast and accurate even in complex detailed faces but could not characterize lips in detailed faces. In the field of image processing, the CoG has been used as well to detect objects. Van Assen et al. in [51] presented a method to localize objects in gray scale images using the CoG. Object location determination was explained using different approaches but the challenge was to determine the exact accurate location in images. Therefore, in [51], the object position was determined first then the CoG technique was used to accurately localize it.

For accurate localization of the CoG of an object, an image is segmented first before calculating the CoG. The work in [52] proposed a method to consider the CoG of polygonal regions in the XY-plane. This method relied on

calculating the CoG from the idea of geometrical conventional instead of using the idea of calculus. The method used *Mathematical* algebra software to expedite the CoG calculations. Meanwhile, [53] presented an algorithm to investigate the accuracy of measuring the velocity and the strength of a magnetic field in the solar photosphere. Their analyses determined that the central wavelength of a spectral line through the CoG was found to be independent of the resolution of the spectral line when the size of the wavelength bridges an important part of the spectral broadening profile. The significance of the CoG was high in every part of the process. Finally, [54] presented a method to use the CoG for explaining the separation between two equal colour values (chromostereopsis). The new method claimed that the human eye can distinguish each colour position at the CoG when the light of the projected colour is diffused. According to their findings, the new method acted better than previous methods.

Summary of the Centre of Gravity

The CoG technique has been used in different fields of life to find the centroid of objects. It was invented and used for real-world objects then adapted to determine the position of objects in images and other situations. Most of the previous approaches investigated in 2D fields; however, approaches that can work up to N-dimension were generally missing. In addition, the conventional calculus formulas particularized were time consuming and inaccurate in some cases. It was required to develop new mathematical formula, especially in image processing, to involve calculus and geometrical properties that can work with 3D data to determine the centre of objects accurately and efficiently.

IV. SURFACE RECONSTRUCTION

The process of surface fitting or curve fitting is the constructing of a surface or curve out of a series of data using a mathematical function. Before we go into the curve and surface fitting technologies, it is good to touch on the description of curves and surfaces in general. Rogers explained in [55] the curve and surface classical technologies such as Bezier, B-Splines, and NURBS. Both curve and surface fitting involve two procedures which represent the main function of fitting. The first is called interpolation, where an exact fit to a series of data is necessitated. The second procedure of fitting is called smoothing, where a function is constructed to approximately fit the data. In different words, the curves and surfaces can be represented explicitly or implicitly. The explicit representation of the form $y = f(x)$ is little used in computer graphics and computer aided design because this type of representation cannot be used for multiple valued functions. Therefore, the implicit representations of the form $f(x, y) = 0$ and $f(x, y, z) = 0$ are more frequently used in computer graphics because they can represent a multiple valued function even though they are still axis dependent, as reported in [55]. Thus, surface or curve fitting is a mathematical or numerical technique used to approximate complex shapes where a best fit to a series of data can be done and in 2D or 3D. Surface and curve fitting have taken much space in history by presenting a tremendous amount of algorithms and approaches and in the different techniques of fitting. The four known techniques of fitting are listed below under a general title of *Spline Fitting Techniques* and a brief explanation of each one of them has been provided according to [55].

A. Spline Fitting Techniques

The spline techniques are the techniques which have been used throughout the history of surface and curve fitting processes. In this field there are four well known and generally used techniques which are briefly explained in this section. The first technique is called Bezier surfaces and curves. The importance of this technique is clearly indicated in the mathematical field of numerical analysis, computer graphics, and other fields. Bezier curve is a parametric curve which can be generalized to higher dimensions known as a Bezier surface and with a special case called a Bezier triangle. The Bezier curves are a vital tool to generate smooth curves. The technique was publicized by a French engineer called *Pierre Bézier* in 1962 to be used to design automobile bodies and it was evaluated in 1959 by *Paul de Casteljau* using *de Casteljau's* algorithm. The Bezier curves are divided into three types depending on the control points. First type is called *Linear Bezier* curves where the curve is actually a straight line between two points and equivalent to linear interpolation. The second type called *Quadratic Bezier* curves are where a curve interpolates three points and constructs a parabolic segment. The third type of Bezier curves called *Cubic Bezier* curves are a curved defined in $\boldsymbol{R^3}$ consisting of four points. A generalization of the Bezier curves is called a Bezier surface where more points can be involved. Fig. 4 illustrates a Bezier curve and its control points.

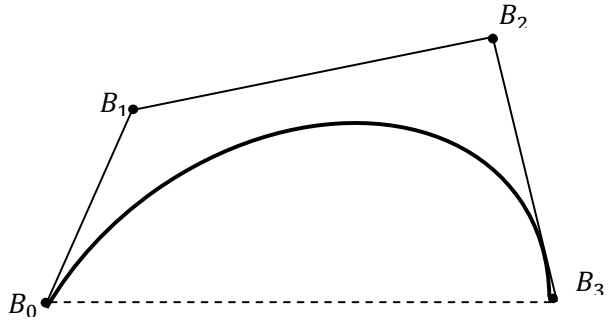

Figure 4. Bezier curve with its control points. [55].

The Bezier curve is important in computer graphics to design 3D surfaces from data obtained from medical or physical objects. The importance of 3D surfaces appears clearly in analysing the surface characteristics. Building 3D surfaces mostly depends on multiple orthogonal curve (e.g. Bezier curve) projections. These details and further information concerning Bezier curves and surfaces are reported in [55].

The second technique is called the B-spline, which was firstly proposed [56]. Splines function, as reported in [55], with a minimal support according to domain partition, smoothness, and degree. Every function of the B-spline can be represented as a combination of linear B-splines of the same degree and smoothness. B-splines are a generalization of Bezier curves and can be evaluated by the *de Boor* algorithm. Types of B-spline are listed here depending on the number of knot spans they represent. First, the *Constant B-spline*, which is not continuous and is defined from only one known span. Second, the *Linear B-spline*, is defined by two knot spans and is continuous. Third, the *Uniform quadratic B-spline*, is a common form of B-spline and is a quadratic B-spline with a uniform knot vector. Fourth, the *Cubic B-spline*, is a set of control points to be represented. Fifth, the *Uniform Cubic B-spline*, is a uniform cubic spline which used commonly in B-spline forms. Each of the previous B-spline types has its own function or evaluation and representation. The B-spline basis which is a special case from Basis splines has a non-global behaviour of B-spline because of the ability to represent each of its vertices by a unique basis function. In addition, the B-splines allow changes to the degree of basis function and, as a result, changing the degree of the curves.

The third technique is called NURBS. This technique, as reported in [55], refers to a Non-Uniform Rational Basis Spline. This mathematical model is generally used in surface and curve fitting in computer graphics and it particularized in its flexibility to handle freeform models. The technique was first used by engineers in the 1950s where a technique that could represent a freeform model such as cars, ship hulls, and aerospace exterior surfaces was needed. NURBS can represent a wide range of curves and surfaces with a single internal representation and form lines and planes to circles and spheres. The NURBS allows the construction of more general surfaces that can make it easy to bury the lines, planes, circles, and spheres in the surface itself. Thus, NURBS besides being robust in representing static objects, it is also efficient in modelling animated characters used in computer games nowadays. Finally, the NURBS are defined by their set of weighted control points and it became clear in 1960s that their generalization are of Bezier splines. It is the standard of much of computer graphics and computer aided design. Fig. 5 below indicates two examples of a NURBS surface with its mesh.

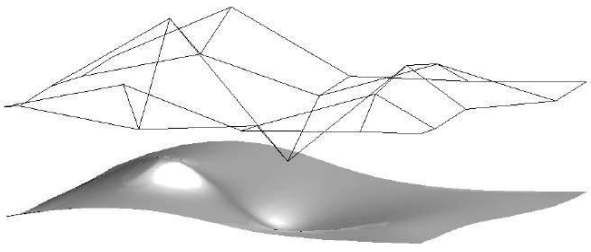

Figure 5. Examples of a NURBS surface with mesh above the surface. [57].

The fourth technique is called Subdivision Surfaces. This technique, as reported in [58], is a repeated refinement process for the 3D control mesh. This method of computer graphics represents smooth surfaces of a rough linear polygon mesh. The subdivision technique can represent a smooth surface from an arbitrary topology type where that surface can be calculated of the recursive subdivision process of each polygonal face into small faces. The B-spline and NURB surfaces suffer from trimming and smoothness problems in some of the commercial geometrical modelling applications. The subdivision surface is one of the best solutions for trimming and sharp edges even though B-spline is easy to analyse since it is piecewise polynomial in form. This process would divide the mesh into new faces and vertices. Fig. 6 below illustrates a subdivision example.

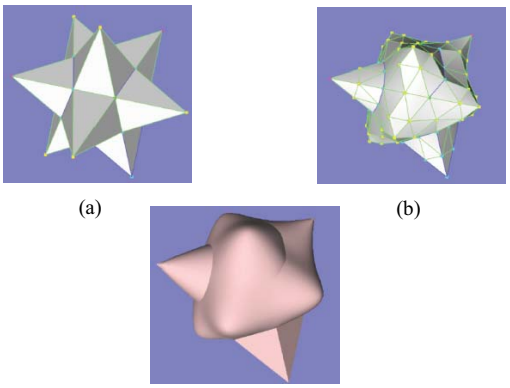

Figure 6. An example of Subdivision surfaces: (a) Initial subdivision surface; (b) refined subdivision surface; (c) The limit surface. [58].

Quite numbers of literatures were presented in the field of surface reconstruction or fitting. The surface fitting approaches have commonly been proposed in 3D data. A research was presented in [59] for surface interpolation in 3D data. The reconstruction process was done globally to control the construction of a surface of a smooth interpolated surface and coarse textures as well. The algorithm was computationally efficient but declared a little limitation in the type of kernel function used. A surface parameterization in 3D medical images of smoothly deformable objects method has been presented in [60]. A global shape parameterization for surfaces was incorporated with a demonstrative parameterized model and was found useful in computer vision and modelling. Good results have been obtained from applying the method into synthetic and real 3D medical images as well. A surface reconstruction algorithm has been demonstrated in [61] to take as input a set of unorganized points. The algorithm develops a smooth surface near scattered points with or without a boundary and in $\boldsymbol{R^3}$. The idea of estimating the distance functions of a zero set determination is proposed in this algorithm. The results showed the correct construction of topologies of all examples presented.

Meanwhile, [62] presented an algorithm whereby the image parameter acquisition was used to evaluate the accuracy of the principal axes and surface fitting on 3D image registration. Two types of phantom objects were used in this algorithm to simulate parts of scans of the acquisition of known parameters. The magnetic resonance (MR) brain images and ellipsoids of defined mathematical representation were used in this algorithm. With this surface fitting method, the results proved to have an accuracy of 1-2 mm to confirm the probability of 3D image registration. Hoppe et al. proposed in [63] a solution to fit a cloud of scattered data after an initial triangulation process in a robust mesh of the same topology as the initial triangulation. Since the number of vertices was small in the output mesh of this algorithm, therefore, the mesh could be used in surface reconstruction of unorganized data and mesh simplification. Medical image registration algorithms have become popular in the field of surface fitting since the increased need to identify anatomical objects in those images has arisen.

Hill and Hawkes in [64] presented a new approach relying on surface fitting to increase the knowledge of determining the anatomical structures in MR CT vascular images of the head. The algorithm proved to have an accurate output to register specified kinds of images and achieve its goals. Hoppe et al. presented in [65] an automatic surface fitting algorithm to fit a cloud of scattered points in smooth surface that could be used in different applications such as reverse engineering. Using subdivision and NURBS approaches, the algorithm clearly demonstrated its ability to recover sharp edges and model a surface out of an arbitrary topology when it was applied to synthetic and real data. In 1996, [66] presented an automatic algorithm for fitting 3D scattered points in B-spline surfaces. Unlike previous approaches, the algorithm considers the surface as a network of B-spline patches and the reconstruction could be done from an arbitrary topology. The algorithm output showed efficient B-spline surfaces. The algorithm had a drawback with a disability of not smoothly reconstructing surfaces with discontinuities such as corners.

A survey paper on interpolating and approximating 3D scattered data onto smooth surfaces has been presented in [67]. The contribution of this paper has distinguished the existing algorithms according to distance functions, warping, spatial subdivision, and the increment in surface growth. The new survey opened a space for new research to be done in this field. In 1997, [68] presented a method to solve the problem of reconstructing the incomplete surfaces extracted from 3D medical images using Radial Basis Functions (RBF). The RBF helped to overcome some restrictions of interpolation geometry. The defects in some objects, such as skulls, could be repaired by the design of implants whereas the method was applied in X-ray CT data obtained by ray tracing techniques. Amenta et al. in [69] developed an algorithm for surface reconstruction of scattered and unorganized 3D data. The algorithm, which was based on a Voronoi diagram, guaranteed good results when a good sample of data was given. A good sample means capturing of intuitive notions to enable the areas with few samples to be reconstructed.

Also in 1998, [70] described a method to smoothly approximate scattered data by preserving a parametric convex Bezier surface. First, a reference surface would be constructed to approximately, not exactly, represent the expected shape. Convexity parameters would be generated depending on the reference surface and then the final approximated surface would be generated by solving a quadratic problem. Regarding the NURBS surfaces, [71] presented an algorithm to reconstruct 3D NURB surfaces from scattered unorganized data. A model was approximated first from the k-means clustering technique and a NURBS network of patches was built from the input scattered data. Secondly, triangulation and polyhedral techniques were used to approximate the arbitrary initial model. The algorithm has given good results and a proposal has been made to apply it to real world 3D video data.

Another algorithm was presented [72] to generate 3D finite element meshes. The generated mesh was for a skewed rotor induction motor depending on its geometrical features and could be rotated in minimal time. The extrusion technique was used to generate the meshes with simplified shapes, i.e., less number of vertices. Amenta et al. in [73] presented an improved algorithm that relied on the crust method developed by the same author two years earlier in [69]. The crust method guaranteed a robust 3D reconstruction of data geometry and topology using a Voronoi diagram and the new algorithm managed to simplify the crust and to prove the homeomorphism of it. The work in [74] presented an approach to reconstruct 3D B-spline surfaces from a scattered data set. The algorithm proposed using the Quadtree data structure method (strip tree) to decompose the input data set into quadratic surfaces. Next, the quadratic surfaces were raised to bi-cubic surfaces to be combined in one B-spline smooth surface. A drawback in the algorithm was the inability to reconstruct twisted surfaces with self-intersecting parts.

A method of Computer Aided Design (CAD) model was presented [75]. The CAD model representation of complicated engineering parts was adopted in this method for the triangulation of 3D unorganized points. The results proved the robustness of the method whereas the triangulation was simplified and enhanced by removing the redundant triangles, smoothing the mesh and removing its stitches. Plenty of current surface reconstruction algorithms perform well on sampled data sets without boundaries detected in these samples. Real data used to perform algorithms comes with part boundary samples and therefore, [76] proposed a new method called *COCONE* to handle the boundary detecting where the sampling ends and undersampling begins. The new method showed to be effective in solving the boundary problem based on some experiments.

Delaunay triangulation is one of the basics in surface reconstruction that has been used in different situations. Thus, [77] proposed a method for surface reconstruction that adopted Delaunay triangulation technique in the work. This technique was shown to be theoretically and practically

effective for surface reconstruction. The predominant issue concerning the Delaunay triangulation is that it cannot handle a large size of data. Therefore, [77] improved the previous *COCONE* algorithm to become the *SUPER COCONE*. Both algorithms (*COCONE* and *SUPER COCONE*) use Delaunay triangulation technique for surface reconstruction. Unlike *COCONE*, *SUPER COCONE* algorithm can handle a large data set.

Surface reconstruction from 3D data sampled from the boundary of an object may generate an arbitrary triangulated mesh. To improve the triangulated mesh and avoid the mesh connectivity computation, an algorithm that was proposed [78] to handle the surface reconstruction process from only the cloud of points. The new algorithm had the ability to reconstruct robust surfaces and represent the steps of coarsely and smoothing. The time-consuming aspect was spared and a new modelling technique for the cloud of points was expressed by using this algorithm. Alexa et al. in [79] proposed a method to use the local maps of differential geometry and Moving Least Square (MLS) to represent a manifold smooth surface quite close to the original surface. The new method was proposed to increase or decrease the density of the cloud of points as well. High quality results have been achieved using this method to produce a smooth reconstruction of silhouettes.

In the meanwhile, [80] have revisited the problem, presenting the *power crust* approach to reconstruct 3D surfaces from points that were sampled from a 3D object. The approach was to produce mesh faces by first approximating the Media Axis Transform (MAT) and then the inverse transform was used to construct the surface. The reconstructed objects were all solid with piecewise-linear manifolds and the outputs were efficient except some holes appeared in some objects. In the meanwhile, [81] has described a fast method to reconstruct 3D smooth surfaces using the RBF out of a cloud of points whereas the implicit zero set of an RBF has been fitted to the cloud of data which belongs to a surface. The output surfaces from the method showed efficiency and smoothness.

As a CAD modification application, [82] presented a method to update CAD models consisting of trimmed or untrimmed surfaces from 3D unorganized points. The proposed method considered the input data as non-uniform and sometimes not covering the whole surface of an object. The results showed a good improvement on time saving and memory requirements. In 2002, [83] presented an algorithm for fitting a surface onto a large scattered data set using subdivision surface techniques. The subdivision surface could be rendered using a hybrid algorithm which was proposed by the same authors. The method proved to have a small approximation error and a robust ability to render large data sets. Measuring the complex surfaces along with their exact mathematical representation have been always difficult to achieve.

However, [84] proposed a method to measure complex surfaces and mathematically represent the surfaces using the Coordinate Measuring Machine (CMM) technique. The method has been used to analyse complex surfaces and make it easier to compare them with other surfaces and it was applied on a known prosthesis for practical evaluation. The point sampling simplification (undersampling) procedure is an important process since the errors that may arise with some surface reconstruction methods are highly to occur. The work in [85] discussed this problem and presented a paper to analyse and quantitatively compare some simplification methods. Fast and robust simplification methods have been presented in that paper to reconstruct high quality surfaces.

Since the problem of surface reconstruction mostly is concentrated in unguaranteed correct topology or data that is geometrically not close to the surface, [86] presented another algorithm for reconstructing water-tight 3D surfaces from unorganized point samples. Since, CAD applications require water-tight surfaces with no holes presented, such an algorithm is a high necessity. The algorithm called *Tight Cocone* required an initial mesh generated by a robust surface reconstruction algorithm to omit holes. The presented results showed a robust ability to reconstruct smooth water-tight surfaces but a drawback appeared from the inability of *Tight Cocone* to reconstruct internal gaps. The appearance of conventional surface fitting techniques has been reduced since the appearance of new more robust approaches after the year 2000. Even so, a few researchers have devoted themselves to improve some of the old algorithms and get them to solve recent problems in surface reconstruction.

Aumann presented in [87] an algorithm to develop a generation of Bezier surfaces using Bezier curves from any shape and degree. Two advantages have been stated using this algorithm: no complicated nonlinear equations have to be solved, and the algorithm could guarantee the singular points to be controllable. From the point of view of surface fitting, samples of cloud data vary from surface to surface and usually the researchers focus on the cloud data obtained from 3D scanner devices. It is worth mentioning that the 3D data acquisition devices sometimes produce a noisy set of data samples whereby those samples do not provide complete information about the scanned surface.

Approaches have been presented to solve such a problem of missing information and one of them was the constructing of a likelihood map to quantify a likelihood set of points for each point in the 3D space that a surface reconstruction might pass through that point. This approach was proposed in [88] to handle a noisy cloud of point samples from real objects. The approach has been merged with a set of scanned samples to construct a new sample set to represent the scanned object and could reconstruct robust surfaces out of the new data sets. The images have been used to reconstruct 3D surfaces in some proposed algorithms in surface fitting as well. The work in [89] presented a surface reconstruction algorithm that relied on images as its input to reconstruct 3D surfaces using the learned shape model technique. The output was robust and coherent with the input image(s).

Most of the approaches that adopt B-spline surface fitting with the least square technique require the measurement of the sensitive parameterization of the cloud of data plus vector knots. Using uniform knots to connect

the points using the data parameterization approach has been proposed in [90]. The proposed technology in that paper provided more parameter features for high curved regions in the space and it could reconstruct even a single B-spline patch. A grid generation over singular trimmed NURBS surfaces using the Floater's algorithm is an approach that has been presented in [91]. The paper explained the approach and how to generate a grid over a four sided trimmed NURBS surface, including a facetted surface as well. In the early 1980s, researchers into digital image processing started investigating the ability to track digital surfaces in 3D images. Chen studied in [92] the surfaces which vary gradually in order to set a suitable algorithm for smooth surface fitting and to generalize the gradually varied surfaces concept in case there is no need for smooth surface fitting of the discrete data.

A new era started after this in terms of surface reconstructing technology and researchers started investigating new approaches to mostly re-form the cloud of data to improve the reconstructed surfaces as a way to save time and memory requirements. The work in [93] presented a novel approach to reconstruct a 3D surface out of 3D orientated points using *Stokes Theorem*. The approach returned solid water-tight 3D surfaces by evaluating the function by zero set concepts, i.e., the function is equal to zero outside the surface and equal to one inside it. The approach was robust in reconstructing 3D models, was fast, and simple in reconstructing water-tight surfaces even with missing or noisy data. Another algorithm for surface reconstruction out of orientated data points was presented in [94]. The new algorithm posited the reconstruction of orientated points as a spatial *Poisson* problem solving. The RBF used to partition the data and blending process was involved afterwards whereas the Poisson technique dealt globally with all points at once. The results have shown robust smooth reconstructed surfaces even from noisy data. In addition, the Poisson approach reduced the processing time for non-huge data but still need some improvement to handle huge amounts of data. In addition, memory requirements have reduced as well using the Poisson approach.

For the importance of Poisson technique in the future of our work, we mention here a brief history about it. There has been wide-ranging research on dealing with Poisson problems and many efficient and robust approaches have been developed. Research appears that the implicit function formulation problem started in the 90's; however, the first practical use of Poisson technique in surface reconstruction was in [94]. Thus, Poisson technique became famous technique for reconstructing water-tight surfaces from oriented data. Poisson earned its great position among all surface reconstruction approaches because it uses a fitting function (implicit function) approach. According to [95], the implicit function combines between local and global fitting schemes. The importance of global that it does not lead to local neighborhoods, selects type of surface patch, and use blend weights. The basis function of Poisson is simply structured for efficient solutions of linear systems. It can deal locally with ambient space rather than the data points.

The basic idea of the Poisson's basis function is to be evaluated near the data points in three ways: less than zero outside the data, larger than zero inside the data, and zero on the borders of the data. Therefore, the key idea is to formulate the oriented data from volume integrals to surface integrals. Unlike other surface reconstruction approaches, spurious sheets are rarely arise with Poisson. This is because the gradient of the integral function (implicit function) is all controlled to the spatial data, [94].

The work in [96] described an improved Poisson algorithm with Marching Cubes algorithm for more generation of realizing representations. The improved algorithm involves more interpolation between the data points and fast searching for more efficient surface reconstruction. In another way, [97] introduced a new formulation for the implicit function of oriented data. This problem attracted a broad attention over two decades for more water-tight surface reconstruction improvement. This work described a simple hybrid algorithm of Poisson problem together with Dual Marching Cubes and Octree partitioning of space. This algorithm preliminary proved of producing accurate and adaptive meshes.

After presenting the *SUPER COCONE* algorithm in 2001, [98] then presented a surface reconstruction algorithm to construct efficient surfaces from data clouds in the presence of reasonable noise. The algorithm was called ROBUST COCONE and it was produced after the COCONE algorithm which worked with noise-free point samples, as described earlier. The robustness of the algorithm was proved by the experimental results but the algorithm might not work well when the level of noise is high.

Surface reconstruction procedures have been applied in different fields and one of these was reverse engineering. Reverse engineering in this context is the building of CAD models using physical parts by measuring the dimensions of each part and performing surface modelling. Dan and Lancheng proposed in [99] a new algorithm for NURBS surface reconstruction for reverse engineering which required less computational processes. The paper described a second new algorithm for scattered point parameterizations. In the same year, [100] presented a robust algorithm for surface reconstruction from a sparse cloud of data by proposing sparse constraints to force the surface to pass through specific points. The surface could be reconstructed from highly sparse points using those constraints.

Another algorithm to construct CAD models from a scattered set of data of free-form objects (unknown topology) has been proposed in [101] based on the NURBS (B-Spline) surface fitting technique. The algorithm was robust at reconstructing NURBS surfaces with optimized patches and the joining of the patches guaranteed the continuity G^1. A robust surface reconstruction process refers to how close the reconstructed surface is compared to the real one. Good reconstructed surfaces require complete and noise-free samples and polygons are usually the best way to reconstruct accurate surfaces out of the measurements obtained. An approach has been presented in [102] to

transfer a laser scanner cloud of points into a 3D model best fit to the real objects with best visualization. The proposed approach through its software called LSM3D proved its reliability in reconstructing architectural models.

In terms of grid generation from 3D data, [103] presented a method to reconstruct real-time grids to best fit a 3D cloud of data which had been derived from different 3D scanners. The output grids have been used to represent NURBS patches to be used in the determination of curvature and quality evaluations. The method has shown robustness in closing grid gaps and with a short processing time. However the only limitation was that the scan-lines could not be overlapped because they might cause a self-overlay in the grids.

In a further improvement on the previously mentioned technique of *Poisson*, [104] presented an algorithm to efficiently undertake the surface reconstruction of a huge amount of data of out-of-core. The same authors of the *Poisson* technique proposed to extend the method to a multi-resolution streaming computation including the Poisson octree data structure solution for the sake of surface reconstruction. An accurate solution was obtained from a single iteration to the multi-resolution pass to handle the global linear system and the algorithm produced a good performance on several huge datasets. The work in [105] proposed the use of the RBF for surface reconstruction in a manner of confidence supported through a proposed software tool. The octree data structure was employed in this algorithm which played a vital role in the reduction of processing time and the handling of huge data sets. A server was made available online to construct surfaces in the Virtual Reality Modelling Language (VRML) file format.

However, [106] presented a curve fitting approach to handle scanned data. Cubic Bezier curves were used to approximate the boundaries of the features of G^1 continuous data. The method proved its effectiveness with a satisfactory accuracy in comparison with other approaches of constructing CAD models. Sharf et al. presented in [107] a 4D space-time surface reconstruction approach out of 3D slices of a solid model bounded by water-tight manifolds. The approach proved its efficiency when it was applied to incomplete data scanned from solid water-tight models. Unlike NURBS surfaces, the subdivision of surfaces of a cloud of points has not been that common in CAD model design. Nevertheless, both the subdivision and NURBS methods have been commonly used to design sculpture shapes.

In the meanwhile, [108] presented a method to employ subdivision geometry and NURBS interpolation to reconstruct a model for reverse engineering by adding a new dimension. The proposed method returned efficient surfaces and the subdivision technique reduced error and time when the data of a structure was good. Most of the previous reviewed surface reconstruction approaches are directly linked to our ideas of proposing a robust surface reconstruction for coronary artery trees. The field of surface reconstruction has a tremendous number of approaches and algorithms; however, the presented works here are part of them and could inspire us to design our own approach.

Continue reviewing, [109] in his thesis described a method to reconstruct 3D surfaces out of scattered points of data obtained by a laser scanner, camera, or a monocular system. Triangular models were constructed for selected areas of the cloud of points, then a set of quads were constructed from the triangulated models. Finally, the quads were translated and approximated to NURBS surfaces. The method dealt well with a cloud of points with less noise even though a clustering technique was used to handle noise and simplify the method. Noise, non-uniform, and outliers (redundant) data are problems that always need to be solved in order to reconstruct smooth and efficient surfaces from a cloud of data. Huang et al. presented in [110] a two-step algorithm to handle these problems and consolidate the scattered data points. First, an operator was employed to project optimally weighted locals to free the cloud of points from noise and redundant-free data. Next, a robust normal estimation framework was employed. The consolidated data acted better than conventional surface reconstruction algorithms thanks to the proposed algorithm.

Bolitho et al. in [95] returned to the problem to present an approach to parallel implement the Poisson algorithm that was proposed earlier by the same authors. The Poisson algorithm adopted the octree data structure technique (multi-grid) in its decomposition and designing. Octree data structure technique gives the ability for the approaches to work in parallel on multi-processors. The parallel processing procedure increased the speed of implementation and improved the memory requirements to be scalable. Most of the previous algorithms proposed surface reconstruction to be based on a scanned cloud of data whereas [111] proposed a robust method for surface reconstruction from merged scans of data sets. The proposed technique to reconstruct the surface in this method was to consider the reconstruction problem as an energy minimization problem and this was the key to constructing models out of the range of images. The proposed method with its combination between a minimization problem and Delaunay triangulation returned robust and water-tight surfaces with an efficient processing time and memory requirements compared to the size of the input data.

In conclusion, Table II below summarizes the algorithms and approaches in the reviewed literature which have been grouped in three categories according to [93].

B. Summary of the Surface Reconstruction

Surface reconstruction using a 3D cloud of data takes up a large proportion of the literature due to the important role that constructing surfaces plays in different fields. It is also worth mentioning here that most of the previous algorithms discuss surface reconstruction from a range of scan data and it is almost unknown to involve surface reconstruction or fitting in modelling objects that have been segmented from 2D medical images and transferred to a 3D cloud of points. The other aspect of interest here is the use of clustering techniques to simplify the cloud of points and reduce noise, therefore, a new procedure could be proposed as a helpful adjunct to be involved in the clustering such as CoG technique.

TABLE II. SURFACE RECONSTRUCTION CATEGORIES

No.	Category	Procedure	Advantages	Limitations
1	The surface reconstruction problem is addressed through the use of computational geometry techniques.	Computing either the Delaunay triangulation of the point samples or the dual Voronoi diagram and using the cells of these structures to define the topological connectivity between the point samples.	- The complexity of the reconstructed surface is in the order of the complexity of the input samples. - It is possible to bound the quality of the reconstruction if the sampling density is known.	- Require the computation of the Delaunay triangulation which can be inefficient for large point samples. - These methods tend to perform less effectively when the point samples are not uniformly distributed over the surface of the model.
2	Methods that address the surface reconstruction problem by directly fitting a surface to the point samples.	The reconstruction problem solved by deforming a base model to optimally fit the input sample points. These approaches represent the base shape as a collection of points with springs between them and adapt the shape by adjusting either the spring stiffness or the point positions as a function of the surface information.	Generating a surface reconstruction whose complexity is in the order of the size of the input samples.	These methods tend to be restrictive as the topology of the reconstructed surface needs to be the same as the topology of the base shape,
3	Methods that address the surface reconstruction problem by fitting a 3D function to the point samples and then extracting the reconstructed surface as an iso-surface of the implicit function.	Reconstructing surfaces using point samples to define an implicit function in 3D and then extract the reconstructed surface as an iso-surface of the function.	- The extracted surface is always guaranteed to be water-tight, returning a model with a well-defined interior and exterior, - The use of an implicit function does not place any restrictions on the topological complexity of the extracted iso-surface, providing a reconstruction algorithm that can be applied to many different 3D models.	The complexity of the reconstruction process is a function of the resolution of the voxel grid, not the output surface, and many of these approaches use hierarchical structures to localize the definition of the implicit function to a thin region about the input samples, thereby reducing both the storage and computational complexity of the reconstruction.

V. CONCLUSION

From the literature review, the indication of the location of coronary arteries of the surface of the heart is a new research problem and as far as we know, it has not been attempted in a separate study before this. Nevertheless, there are plenty of studies involving the steps of solving the problem of vessel extraction, 3D reconstruction, centre of gravity, and surface reconstruction or fitting. For the vessel extraction technologies, there are no preferred techniques that have been chosen as basic vessel extraction approaches and the combination with various improvements of some of these techniques could be robust and fast enough to fit the needs of the work of my PhD work. In terms of 3D reconstruction, most of the previous algorithms adopted the multi-image approach and sometimes bi-plane angiogram images to reconstruct a 3D view. A robust approach needs a faster algorithm that works with a reduced number of images (single-view) and consequently less images means a decrease in radiation exposure and a reduced likelihood of endangering the lives of patients. Finally, the surface reconstruction technique had been extremely well discussed in the literature but no separate study has been proposed to handle coronary artery tree surface reconstruction. The direct way has been to use algorithms that can offer faster processing, reduced memory requirements, and can return smooth and efficient surfaces. Therefore, methods that address the surface reconstruction problem as an evaluation of an implicit function to construct iso-surfaces have been chosen as the methods of choice.

REFERENCES

[1] C. Y. Lin and Y. T. Ching, "Extraction of coronary arterial tree using cine X-ray angiograms," *BIOMEDICAL ENGINEERING APPLICATIONS BASIS COMMUNICATIONS*, vol. 17, no. 3, p. 111, 2005.

[2] C. Kose and C. Ikibas, "Segmentation of coronary vessel structures in X-ray angiogram images by using spatial pattern matching method," IEEE, 2008, pp. 1-6.

[3] C. Kirbas and F. Quek, "A review of vessel extraction techniques and algorithms," *ACM Computing Surveys*, vol. 36, no. 2, pp. 81-121, 2004.

[4] F. Novoa, ., A. Curra, M. G. L≤pez, and V. Mato, "Angiographic Images Segmentation Techniques," *Encyclopedia of artificial intelligence*, p. 110, 2009.

[5] J. F. Canny, "Finding edges and lines in images," *Massachusetts Inst. of Tech. Report*, vol. 1 1983.

[6] P. H. Eichel, E. J. Delp, K. Koral, and A. J. Buda, "A method for a fully automatic definition of coronary arterial edges from cineangiograms," *Medical Imaging, IEEE Transactions on*, vol. 7, no. 4, pp. 313-320, 1988.

[7] A. D. Hoover, V. Kouznetsova, and M. Goldbaum, "Locating blood vessels in retinal images by piecewise threshold probing of a matched filter response," *Medical Imaging, IEEE Transactions on*, vol. 19, no. 3, pp. 203-210, 2000.

[8] S. Chaudhuri, S. Chatterjee, N. Katz, M. Nelson, and M. Goldbaum, "Detection of blood vessels in retinal images using two-dimensional matched filters," *Medical Imaging, IEEE Transactions on* , vol. 8, no. 3, pp. 263-269, 1989.

[9] Y. Sun, "Automated identification of vessel contours in coronary arteriograms by an adaptive tracking algorithm," *Medical Imaging, IEEE Transactions on*, vol. 8, no. 1, pp. 78-88, 1989.

[10] B. Cote, W. Hart, M. Goldbaum, P. Kube, and M. Nelson, "Classification of blood vessels in ocular fundus images," *Computer Science and Engineering Dept. , Univ. of California, San Diego, Tech Rep*, 1994.

[11] S. Aylward, J. Coggins, T. Cizadlo, and N. Andreasen, "Spatially invariant classification of tissues in MR images," Citeseer, 1994.

[12] S. Aylward, S. Pizer, D. Eberly, and E. Bullitt, "Intensity ridge and widths for tubular object segmentation and description," Published by the IEEE Computer Society, 1996, p. 0131.

[13] H. Greenspan, M. Laifenfeld, S. Einav, and O. Barnea, "Evaluation of center-line extraction algorithms in quantitative coronary angiography," *Medical Imaging, IEEE Transactions on*, vol. 20, no. 9, pp. 928-941, 2001.

[14] S. R. Aylward and E. Bullitt, "Initialization, noise, singularities, and scale in height ridge traversal for tubular object centerline extraction," *Medical Imaging, IEEE Transactions on*, vol. 21, no. 2, pp. 61-75, 2002.

[15] D. Yi and V. Hayward, "Skeletonization of volumetric angiograms for display," *Computer Methods in Biomechanics and Biomedical Engineering*, vol. 5, no. 5, pp. 329-341, 2002.

[16] S. Wesarg and E. A. Firle, "EA: Segmentation of Vessels: The Corkscrew Algorithm," *SPIE International Symposium on Medical Imaging*, 2004.

[17] V. Mahadevan, H. Narasimha-Iyer, B. Roysam, and H. L. Tanenbaum, "Robust model-based vasculature detection in noisy biomedical images," *Information Technology in Biomedicine, IEEE Transactions on*, vol. 8, no. 3, pp. 360-376, 2004.

[18] Y. Wang, H. Z. Shu, Z. D. Zhou, C. Toumoulin, and J. L. Coatrieux, "Vessel extraction in coronary X-ray Angiography," IEEE, 2005, pp. 1584-1587.

[19] Y. Xu, H. Zhang, H. Li, and G. Hu, "An improved algorithm for vessel centerline tracking in coronary angiograms," *Computer methods and programs in biomedicine*, vol. 88, no. 2, pp. 131-143, 2007.

[20] C. Li, C. Y. Kao, J. C. Gore, and Z. Ding, "Minimization of region-scalable fitting energy for image segmentation," *Image Processing, IEEE Transactions on*, vol. 17, no. 10, pp. 1940-1949, 2008.

[21] W. C. K. Wong and A. C. S. Chung, "Principal curves to extract vessels in 3D angiograms," 2008.

[22] C. Bauer and H. Bischof, "Edge Based Tube Detection for Coronary Artery Centerline Extraction," *The Insight Journal*, 2008.

[23] P. T. H. Truc, M. A. U. Khan, Y. K. Lee, S. Lee, and T. S. Kim, "Vessel enhancement filter using directional filter bank," *Computer Vision and Image Understanding*, vol. 113, no. 1, pp. 101-112, 2009.

[24] J. A. Fessler and A. Macovski, "Object-based 3-D reconstruction of arterial trees from magnetic resonance angiograms," *Medical Imaging, IEEE Transactions on*, vol. 10, no. 1, pp. 25-39, 1991.

[25] A. Wahle, H. Oswald, and E. Fleck, "3D heart-vessel reconstruction from biplane angiograms," *Computer Graphics and Applications, IEEE*, vol. 16, no. 1, pp. 65-73, 1996.

[26] T. Saito, M. Misaki, K. Shirato, and T. Takishima, "Three-dimensional quantitative coronary angiography," *Biomedical Engineering, IEEE Transactions on*, vol. 37, no. 8, pp. 768-777, 1990.

[27] T. Kayikcioglu and S. Mitra, "A new method for estimating dimensions and 3-d reconstruction of coronary arterial trees from biplane angiograms," IEEE, 1993, pp. 153-158.

[28] A. Wahle, E. Wellnhofer, H. Oswald, and E. Fleck, "Biplane coronary angiography: Accurate quantitative 3-D reconstruction without isocenter," IEEE, 1993, pp. 97-100.

[29] T. V. Nguyen and J. Sklansky, "Reconstructing the 3-D medial axes of coronary arteries in single-view cineangiograms," *Medical Imaging, IEEE Transactions on*, vol. 13, no. 1, pp. 61-73, 1994.

[30] Y. Sato, S. Nakajima, H. Atsumi, T. Koller, G. Gerig, S. Yoshida, and R. Kikinis, "3D multi-scale line filter for segmentation and visualization of curvilinear structures in medical images," Springer, 1998, pp. 213-222.

[31] S. J. Chen and J. D. Carroll, "3-D reconstruction of coronary arterial tree to optimize angiographic visualization," *Medical Imaging, IEEE Transactions on*, vol. 19, no. 4, pp. 318-336, 2000.

[32] L. Sarry and J. Y. Boire, "Three-dimensional tracking of coronary arteries from biplane angiographic sequences using parametrically deformable models," *Medical Imaging, IEEE Transactions on* , vol. 20, no. 12, pp. 1341-1351, 2001.

[33] A. Sarwal and A. Dhawan, "Three dimensional reconstruction of coronary arteries from two views,", 2 ed IEEE, 2001, pp. 565-568.

[34] S. Y. J. Chen, J. D. Carroll, and J. C. Messenger, "Quantitative analysis of reconstructed 3-D coronary arterial tree and intracoronary devices," *Medical Imaging, IEEE Transactions on*, vol. 21, no. 7, pp. 724-740, 2002.

[35] E. Wellnhofer, A. Wahle, and E. Fleck, "Progression of coronary atherosclerosis quantified by analysis of 3-D reconstruction of left coronary arteries," *Atherosclerosis*, vol. 160, no. 2, pp. 483-493, 2002.

[36] R. N. Ghanem, C. Ramanathan, P. Jia, and Y. Rudy, "Heart-surface reconstruction and ECG electrodes localization using fluoroscopy, epipolar geometry and stereovision: application to noninvasive imaging of cardiac electrical activity," *Medical Imaging, IEEE Transactions on*, vol. 22, no. 10, pp. 1307-1318, 2003.

[37] D. Sherknies, J. Meunier, and J. C. Tardif, "3D heart motion from single-plane angiography of the coronary vasculature: a model-based approach,", 5370 ed 2004, p. 381.

[38] K. R. Hoffmann, A. M. Walczak, and P. B. Noel, "3D reconstruction of the carotid artery from two views using a single centerline,", 1268 ed Elsevier, 2004, pp. 177-182.

[39] C. V. Bourantas, I. C. Kourtis, M. E. Plissiti, D. I. Fotiadis, C. S. Katsouras, M. I. Papafaklis, and L. K. Michalis, "A method for 3D reconstruction of coronary arteries using biplane angiography and intravascular ultrasound images," *Computerized Medical Imaging and Graphics*, vol. 29, no. 8, pp. 597-606, 2005.

[40] C. Blondel, G. Malandain, R. Vaillant, and N. Ayache, "Reconstruction of coronary arteries from a single rotational X-ray projection sequence," *Medical Imaging, IEEE Transactions on*, vol. 25, no. 5, pp. 653-663, 2006.

[41] J. Lee, P. Beighley, E. Ritman, and N. Smith, "Automatic segmentation of 3D micro-CT coronary vascular images," *Medical image analysis*, vol. 11, no. 6, pp. 630-647, 2007.

[42] D. Mueller, A. Maeder, and P. OShea, "Tagged volume rendering of the heart," *Medical Image Computing and Computer-Assisted InterventionûMICCAI 2007*, pp. 194-201, 2007.

[43] A. Zifan, P. Liatsis, P. Kantartzis, M. Gavaises, N. Karcanias, and D. Katritsis, "Automatic 3D Reconstruction of Coronary Artery Centerlines from Monoplane X-ray Angiogram Images," *International Journal of Biological and Medical Sciences*, vol. 1, no. 1, pp. 44-49, 2008.

[44] M. Ohta, "Three-Dimensional Reconstruction of a Cerebral Stent using Micro-CT for Computational Simulation," *Journal of Intelligent Material Systems and Structures*, vol. 19, no. 3, p. 313, 2008.

[45] G. A. ten Brinke, C. H. Slump, and C. J. Storm, "Bi-Plane X-ray coronary 3D reconstruction for flow velocity assessment," 2009.

[46] C. Rohkohl, G. Lauritsch, A. Keil, and J. Hornegger, "CAVAREVùan open platform for evaluating 3D and 4D cardiac vasculature reconstruction," *Physics in Medicine and Biology*, vol. 55, p. 2905, 2010.

[47] J. E. Arlot, "The determination of the center of gravity of a planet from photographic plates," *Celestial Mechanics and Dynamical Astronomy*, vol. 26, no. 2, pp. 199-205, 1982.

[48] E. D. Lemaire, M. Lamontagne, H. W. Barclay, T. John, and G. Martel, "A technique for the determination of center of gravity and rolling resistance for tilt-seat wheelchairs," *J Rehabil Res Dev*, vol. 28, no. 3, pp. 51-58, 1991.

[49] A. Patwardhan, "Subpixel position measurement using 1D, 2D and 3D centroid algorithms with emphasis on applications in confocal microscopy," *Journal of Microscopy*, vol. 186, no. 3, pp. 246-257, 1997.

[50] J. Miao, W. Gao, Y. Chen, and J. Lu, "Gravity-center template based human face feature detection," *Advances in Multimodal InterfacesùICMI 2000*, pp. 207-214, 2000.

[51] H. C. Van Assen, M. Egmont-Petersen, and J. H. C. Reiber, "Accurate object localization in gray level images using the center of gravity measure: accuracy versus precision," *Image Processing, IEEE Transactions on*, vol. 11, no. 12, pp. 1379-1384, 2002.

[52] T. de Alwis, "The Center of Gravity of Plane Regions and Ruler and Compass Constructions," 2002.

[53] H. Uitenbroek, "The accuracy of the center-of-gravity method for measuring velocity and magnetic field strength in the solar photosphere," *The Astrophysical Journal*, vol. 592, p. 1225, 2003.

[54] A. Kitaoka, I. Kuriki, and H. Ashida, "The center-of-gravity model of chromostereopsis," *Ritsumeikan Journal of Human Sciences*, vol. 11, pp. 59-64, 2006.

[55] D. F. Rogers, *An introduction to NURBS: with historical perspective* Morgan Kaufmann, 2001.

[56] I. J. Schoenberg, "Contributions to the problem of approximation of equidistant data by analytic functions," *Quart. Appl. Math*, vol. 4, no. part A, pp. 45-99, 1946.

[57] C. W. Anderson and S. Crawford-Hines, "Fast generation of nurbs surfaces from polygonal mesh models of human anatomy," *Technical Report CS-99-101, Colorado State University*, 2000.

[58] J. E. Schweitzer, C. Supervisory, and A. D. Derose, "Analysis and application of subdivision surfaces," 1996.

[59] G. B. Smith and SRI International.Artificial Intelligence Center.Computer Science and Technology Division, "A fast surface interpolation technique," SRI INTERNATIONAL MENLO PARK CA ARTIFICIAL INTELLIGENCE CENTER, 1984.

[60] L. H. Staib and J. S. Duncan, "Deformable Fourier models for surface finding in 3-D images," Citeseer, 1992, p. 90.

[61] H. H. Tony, T. Derose, T. Duchamp, J. Mcdonald, and W. Stuetzle, "Surface Reconstruction from Unorganized Points," 1992.

[62] H. Rusinek, W. H. Tsui, A. V. Levy, M. E. Noz, and M. J. de Leon, "Principal axes and surface fitting methods for three-dimensional image registration," *Journal of nuclear medicine*, vol. 34, no. 11, p. 2019, 1993.

[63] H. Hoppe, T. Derose, T. Duchamp, J. Mcdonald, and W. Stuetzle, "Mesh optimization," ACM, 1993, pp. 19-26.

[64] D. L. G. Hill and D. J. Hawkes, "Medical image registration using knowledge of adjacency of anatomical structures," *Image and Vision Computing*, vol. 12, no. 3, pp. 173-178, 1994.

[65] H. Hoppe, T. Derose, T. Duchamp, M. Halstead, H. Jin, J. Mcdonald, J. Schweitzer, and W. Stuetzle, "Piecewise smooth surface reconstruction," ACM, 1994, pp. 295-302.

[66] M. Eck and H. Hoppe, "Automatic reconstruction of B-spline surfaces of arbitrary topological type," ACM, 1996, pp. 325-334.

[67] R. Mencl and H. Muller, "Interpolation and approximation of surfaces from three-dimensional scattered data points," IEEE, 1997, p. 223.

[68] J. C. Carr, W. R. Fright, and R. K. Beatson, "Surface interpolation with radial basis functions for medical imaging," *IEEE Transactions on Medical Imaging*, vol. 16, no. 1, pp. 96-107, 1997.

[69] N. Amenta, M. Bern, and M. Kamvysselis, "A new Voronoi-based surface reconstruction algorithm," ACM, 1998, pp. 415-421.

[70] B. Jiittler, "Convex Surface Fitting with Parametric Bθzier Surfaces," 1998.

[71] I. K. Park, S. U. Lee, and I. D. Yun, "Constructing NURBS surface model from scattered and unorganized range data," Published by the IEEE Computer Society, 1999, p. 0312.

[72] S. L. Ho, W. N. Fu, and H. C. Wong, "Generation and rotation of 3-D finite element mesh for skewed rotor induction motors using extrusion technique," *Magnetics, IEEE Transactions on*, vol. 35, no. 3, pp. 1266-1269, 1999.

[73] N. Amenta, S. Choi, T. K. Dey, and N. Leekha, "A simple algorithm for homeomorphic surface reconstruction," ACM, 2000, pp. 213-222.

[74] B. F. Gregorski, B. Hamann, and K. I. Joy, "Reconstruction of B-spline surfaces from scattered data points," IEEE, 2002, pp. 163-170.

[75] M. Ristic, D. Brujic, and S. Handayani, "Triangulation of unordered data using trimmed NURBS computer aided design models," *Proceedings of the Institution of Mechanical Engineers, Part B: Journal of Engineering Manufacture*, vol. 214, no. 6, pp. 509-514, 2000.

[76] T. K. Dey and J. Giesen, "Detecting undersampling in surface reconstruction," ACM, 2001, pp. 257-263.

[77] T. K. Dey, J. Giesen, and J. Hudson, "Delaunay based shape reconstruction from large data," IEEE, 2001, pp. 19-146.

[78] L. Linsen, *Point cloud representation* Univ., Fak. f_r Informatik, Bibliothek, 2001.

[79] M. Alexa, J. Behr, D. Cohen-Or, S. Fleishman, D. Levin, and C. T. Silva, "Computing and rendering point set surfaces," *IEEE Transactions on Visualization and Computer Graphics*, vol. 9, no. 1, pp. 3-15, 2003.

[80] N. Amenta, S. Choi, and R. K. Kolluri, "The power crust," ACM, 2001, pp. 249-266.

[81] J. C. Carr, R. K. Beatson, J. B. Cherrie, T. J. Mitchell, W. R. Fright, B. C. McCallum, and T. R. Evans, "Reconstruction and representation of 3D objects with radial basis functions," ACM, 2001, pp. 67-76.

[82] D. Brujic, M. Ristic, and I. Ainsworth, "Measurement-based modification of NURBS surfaces," *Computer-Aided Design*, vol. 34, no. 3, pp. 173-183, 2002.

[83] V. Scheib, J. Haber, M. C. Lin, and H. P. Seidel, "Efficient fitting and rendering of large scattered data sets using subdivision surfaces,", 21 ed John Wiley & Sons, 2002, pp. 353-362.

[84] R. Wirza, M. Bloor, and J. Fisher, "Inspection Strategies for Complex Curved Surfaces Using CMM," *Computational ScienceùICCS 2002*, pp. 184-193, 2002.

[85] M. Pauly, M. Gross, and L. P. Kobbelt, "Efficient simplification of point-sampled surfaces," IEEE, 2002, pp. 163-170.

[86] T. K. Dey and S. Goswami, "Tight cocone: a water-tight surface reconstructor," *Journal of Computing and Information Science in Engineering*, vol. 3, p. 302, 2003.

[87] G. Aumann, "A simple algorithm for designing developable Bezier surfaces," *Computer Aided Geometric Design*, vol. 20, no. 8-9, pp. 601-619, 2003.

[88] M. Pauly, N. J. Mitra, and L. J. Guibas, "Uncertainty and variability in point cloud surface data,", 84 ed Citeseer, 2004.

[89] J. E. Solem and F. Kahl, "Surface reconstruction using learned shape models," *Advances in Neural Information Processing Systems*, vol. 17, p. 1, 2005.

[90] L. Yu-kun, H. Shi-min, and H. Pottmann, "Surface fitting based on a feature sensitive parametrization," *Computer-Aided Design*, vol. 38, no. 7, pp. 800-807, 2005.

[91] S. Gopalsamy, D. Ross, Y. Ito, and A. Shih, "Structured Grid Generation over NURBS and Facetted Surface Patches by Reparametrization," Springer, 2005, pp. 287-299.

[92] L. Chen, "Gradually varied surfaces and gradually varied functions," 2005.

[93] M. Kazhdan, "Reconstruction of solid models from oriented point sets," Eurographics Association, 2005, p. 73.

[94] M. Kazhdan, M. Bolitho, and H. Hoppe, "Poisson surface reconstruction," Eurographics Association, 2006, pp. 61-70.

[95] M. Bolitho, M. Kazhdan, R. Burns, and H. Hoppe, "Parallel Poisson surface reconstruction," *Advances in Visual Computing*, pp. 678-689, 2009.

[96] X. Li, W. Wan, X. Cheng, and B. Cui, "An improved Poisson Surface Reconstruction algorithm," IEEE, 2010, pp. 1134-1138.

[97] F. Calakli and G. Taubin, "SSD: Smooth Signed Distance Surface Reconstruction,", 30 ed Wiley Online Library, 2011, pp. 1993-2002.

[98] T. K. Dey and S. Goswami, "Provable surface reconstruction from noisy samples," *Computational Geometry*, vol. 35, no. 1-2, pp. 124-141, 2006.

[99] J. Dan and W. Lancheng, "An algorithm of NURBS surface fitting for reverse engineering," *The International Journal of Advanced Manufacturing Technology*, vol. 31, no. 1, pp. 92-97, 2006.

[100] J. E. Solem, "Variational surface interpolation from sparse point and normal data," *IEEE transactions on pattern analysis and machine intelligence*, pp. 181-184, 2006.

[101] J. W. Branch, F. Prieto, and P. Boulanger, "Automated Reverse Engineering of Free Form Objects Using Morse Theory," 2007.

[102] D. Gonzβlez-Aguilera, P. Rodrىguez-Gonzβlvez, and J. G≤mez-Lahoz, "An automatic procedure for co-registration of terrestrial laser scanners and digital cameras," *ISPRS Journal of Photogrammetry and Remote Sensing*, vol. 64, no. 3, pp. 308-316, 2007.

[103] C. Teutsch, D. Berndt, E. Trostmann, and B. Preim, "Adaptive Real-Time Grid Generation from 3D Line Scans for fast Visualization and Data Evaluation," 2007.

[104] M. Bolitho, M. Kazhdan, R. Burns, and H. Hoppe, "Multilevel streaming for out-of-core surface reconstruction," Eurographics Association, 2007, pp. 69-78.

[105] N. Kojekine, V. Savchenko, D. Berzin, and I. Hagiwara, "Software tools for compactly supported radial basis functions," *Computer Graphics and Imaging, Proc. IASTED CGIM2000, Hawaii, USA, August*, pp. 13-16, 2008.

[106] V. Stamati and I. Fudos, "On Reconstructing 3D Feature Boundaries," 2008.

[107] A. Sharf, D. A. Alcantara, T. Lewiner, C. Greif, A. Sheffer, N. Amenta, and D. Cohen-Or, "Space-time surface reconstruction using incompressible flow," *ACM Transactions on Graphics (TOG)*, vol. 27, no. 5, pp. 1-10, 2008.

[108] P. Pal, "A reconstruction method using geometric subdivision and NURBS interpolation," *The International Journal of Advanced Manufacturing Technology*, vol. 38, no. 3, pp. 296-308, 2008.

[109] J. Lankinen, "3D Surface Modeling From Point Clouds." 2009.

[110] H. Huang, D. Li, H. Zhang, U. Ascher, and D. Cohen-Or, "Consolidation of unorganized point clouds for surface reconstruction," *ACM Transactions on Graphics (TOG)*, vol. 28, no. 5, pp. 1-7, 2009.

[111] P. Labatut, J. P. Pons, and R. Keriven, "Robust and efficient surface reconstruction from range data,", 28 ed Wiley Online Library, 2009, pp. 2275-2290.